Inorganica Chimica Acta, *122* (1986) 249–253

Anhydrous Lanthanide Chlorides Doped Rare-earth Polyacetylene

ZHONGXIN CHEN and ZHIQUAN SHEN

Department of Chemistry, Zhejiang University, Hangzhou, China

(Received July 25, 1986)

Abstract

Lanthanide chlorides ($LnCl_3$) of all fifteen rare-earth elements, except Pm, have been used as new dopants for the chemical doping of rare-earth polyacetylene (PA) films. The doping reaction takes place in a saturated tetrahydrofuran solution of $LnCl_3$. The doped PA films exhibit an increase of 1–3 orders in conductivity as compared with the undoped one and, moreover, can be used as good substrates for the redoping with $FeCl_3$ or I_2 to prepare films having high and more stable conductivity. Characterizations using techniques of infrared spectrophotometry, electron spin resonance, differential scanning calorimetry and X-ray diffraction have also been performed for the resultant PA. It is demonstrated by the physical characterizations that the dopant species are partially coordinated to the PA chains but have no significant influence on the PA structure.

Introduction

New dopants other than the commonly used halogen, AsF_5 and SbF_5 compounds have recently been explored for the doping of PA. While much work was carried out using metal halides in the d- or p-family such as $FeCl_3$, $AlCl_3$ and $CuCl_2$ as the dopants for PA [1–3], only a few reports have briefly mentioned the use of f-family metal chlorides–lanthanide chlorides ($LnCl_3$) [4]. In the present work a systematic study about the chemical doping of rare-earth PA films with all 15 lanthanide chlorides has been carried out. The doped PA was characterized by employing d.c. electrical conductivity measurements, infrared spectrophotometry (IR), differential scanning calorimetry (DSC), electron spin resonance (ESR) and X-ray diffraction study.

Experimental

Synthesis

High *cis*-(~95%) rare-earth PA films were synthesized by the polymerization of acetylene using a coordination catalyst of neodymium naphthenate–triisobutyl aluminium [$Nd(naph)_3$–$Al(i\text{-}C_4H_9)_3$] at room temperature as reported previously [5]. *Trans*-PA was obtained by the thermal isomerization of *cis*-PA *in vacuo*. The thickness of the PA samples was *ca.* 40 μm. Anhydrous lanthanides were prepared according to the method described in ref. [6].

Doping

The doping of PA with $LnCl_3$ was carried out by immersing PA films in various saturated solutions of $LnCl_3$ under inert atmosphere. All solvents, except H_2O and ethanol, were predried and distilled before use. After doping the film was washed with pure solvent and then vacuum dried. The composition of the doped PA was assumed to be $[CH(LnCl_3)_y]_x$, where y represents the dopant concentration in molar ratio and was obtained by weight uptake.

Characterization

The d.c. electrical conductivity of *cis*- and *trans*-PA (doped and undoped) was measured by a ZC-36 ultrahigh resistivity measurement meter and the two-probe technique, respectively. The DSC diagram was recorded by a CDR-1 calorimeter. Instruments and techniques used for IR spectroscopy, ESR measurements and X-ray diffraction study were the same as in ref. 7.

Results and Discussion

Effect of Solvent Type on the Doping

A study of the solvent effect on $LnCl_3$ doping of PA has been carried out by using various saturated doping solutions of $LnCl_3$ in solvents including water, ethanol, toluene, trichloromethane, tetrahydrofuran-(THF), acetone, nitromethane and some binary solvent mixtures. It was found that the doping reaction takes place in $LnCl_3$ solutions of THF, acetone, trichloromethane and in binary mixtures of acetone/THF, nitromethane/THF, acetone/nitromethane (volume ratio: 1:1). Dopant concentrations can be controlled by the doping period in these cases. No cooperative effects are found in mixed solvents. Some of the results are listed in Table I.

0020-1693/86/$3.50

TABLE I. Influence of Solvent on the Doping Effect of PA by $LnCl_3$[a]

Solvent		THF	Nitromethane	Nitromethane/THF	Nitromethane/Acetone
$[CH(LnCl_3)_y]_x$	Ln = Sm	0.0356	0	0.0400	0.0147
y	Ln = Y	0.0271	0	0.0123	0.0100

[a]Doping period: 50 h.

A small amount of water is absorbed by the dopants of $LnCl_3$ in doped PA as two vibrational bands around 3200 cm^{-1} (HOH stretch) and 1620 cm^{-1} (HOH bend) [8], as shown in the IR spectrum for $SmCl_3$ doped PA (Fig. 1a, b). These two bands are very weak when THF is used as the doping solvent. Therefore, we chose the THF solution of $LnCl_3$ for the following study. Moreover, since no difference except for the HOH vibrational bands is observed in the IR spectra between the PA films doped in the different solvents as shown in Fig. 1a, b, it can be suggested that only the $LnCl_3$ species penetrates into the PA film, even though some amount of $LnCl_3 \cdot n$THF complexes exist in a $LnCl_3$/THF solution [9].

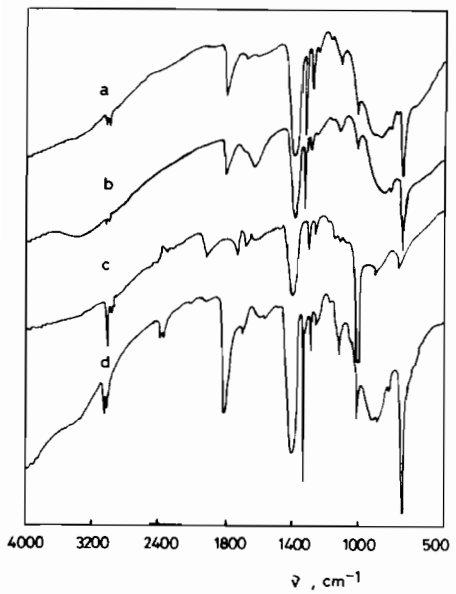

Fig. 1. Infrared spectra of $LnCl_3$ doped PA–$[CH(LnCl_3)_y]_x$. (a) *cis*-$(CH)_x$ Ln = Sm y = 0.0356; (b) *cis*-$(CH)_x$ Ln = Sm y = 0.0426; (c) *trans*-$(CH)_x$ Ln = Sm y = 0.0043; (d) *cis*-$(CH)_x$ Ln = Ho y = 0.0041. Samples a, c, d were obtained by doping in a THF solution of $SmCl_3$ or $HoCl_3$ and sample b in a acetone solution of $SmCl_3$.

Conductivity of the $LnCl_3$ Doped PA

The $SmCl_3$ doped PA gives a large increase in conductivity initially even when the dopant concentration is small (y = 0.0014). Then the conductivity increases slowly with further increase of the dopant concentration, as seen in Table II. Such a result may be explained by the fact that $LnCl_3$ compounds are poor p-type dopants for PA according to the reduction potential theory by MacDiarmid *et al.* [10].

Table III lists the d.c. electrical conductivity values of *cis*- and *trans*-PA films doped with $LnCl_3$ for all fifteen rare-earth elements under comparable conditions. No significant difference is revealed among these doped PA films, which may be due to the similarity of chemical properties for all $LnCl_3$ compounds.

Although these $LnCl_3$ doped PA films exhibit low conductivities, they can be used as good substrates for redoping with $FeCl_3$ or I_2 to prepare PA films having high conductivity. The conductivity of these films decays very slowly while they are stored in dry air at ambient temperature, as shown in Table IV; this demonstrates that the conductivity stability of PA can be achieved by predoping PA films with $LnCl_3$ before doping with $FeCl_3$ or I_2.

Characterization of the $LnCl_3$ Doped PA

IR spectroscopy

The infrared spectra of the $SmCl_3$ doped PA films show that a sharp peak appears at 1298 cm^{-1} (for *cis*-PA) or becomes stronger (for *trans*-PA), besides the appearance of two characteristic doping bands around 1400 cm^{-1} and 900 cm^{-1} (Fig. 1a, c). It is

TABLE II. Conductivity of the $SmCl_3$ Doped PA–$[CH(SmCl_3)_y]_x$[a]

cis-$(CH)_x$	y	0.0014	0.0029	0.0064	0.0134	0.0223	0.0498
	$\sigma \times 10^9$ (Ω^{-1} cm^{-1})	4.3	1.5	7.8	6.0	15	2.3
trans-$(CH)_x$	y	0.0023	0.0043	0.0065	0.0364		
	$\sigma \times 10^4$ (Ω^{-1} cm^{-1})	1.3	2.4	1.4	1.6		

[a]Pristine *cis*-$(CH)_x$ $\sigma_0 = 2.8 \times 10^{-11}$ Ω^{-1} cm^{-1}; *trans*-$(CH)_x$ $\sigma_0 = 1.8 \times 10^{-5}$ Ω^{-1} cm^{-1}.

TABLE III. Conductivity and Dopant Concentrations of PA films Doped with $LnCl_3$ of All Fifteen Rare-earth Elements[a]

$[CH(LnCl_3)_y]_x$		La	Ce	Pr	Nd	Sm	Eu	Gd	Tb
cis-	y	0.0304	0.0204	0.172	0.0192	0.0498	0.0068	0.0070	0.0097
	$\sigma/\Omega^{-1}\,cm^{-1}$ ($\times10^9$)	7.6	1.42	21.0	7.6	2.33	1.11	0.59	0.51
trans-	y	0.0330	0.0200	0.102	0.0510	0.0364	0.0076	0.0112	0.0064
	$\sigma/\Omega^{-1}\,cm^{-1}$ ($\times10^5$)	0.96	1.34	1.46	2.0	1.64	1.15	1.08	1.04
$[CH(LnCl_3)_y]_x$		Dy	Ho	Er	Tm	Yb	Lu	Y	
cis-	y	0.0390	0.0112	0.0112	0.0249	0.0192	0.0353	0.0136	
	$\sigma/\Omega^{-1}\,cm^{-1}$ ($\times10^9$)	1.6	6.47	1.63	9.70	3.00	4.3	2.4	
trans-	y	0.0247	0.0065	0.0068	0.0172	0.0191	0.0263	0.0515	
	$\sigma/\Omega^{-1}\,cm^{-1}$ ($\times10^5$)	3.46	0.48	0.54	0.99	0.95	1.37	2.08	

[a]Doping conditions: 50 h, 22 °C.

TABLE IV. Conductivity Decay of Various Doped PA Films with Storage under Dry Air

		$\sigma/(\Omega^{-1}\,cm^{-1})$							
Sample	Time (days):	0	4	7	12	18	24	35	69
$[CH(FeCl_4)_{0.0508}]_x$		807	748	676		619	615	549	347
$[CH(SmCl_3)_{0.0019}I_{0.130}]_x$		198	184	162	178	159	118	65	42
$[CH(SmCl_3)_{0.0019}(FeCl_4)_{0.0502}]_x$		493	449	465	481	452	436	366	310

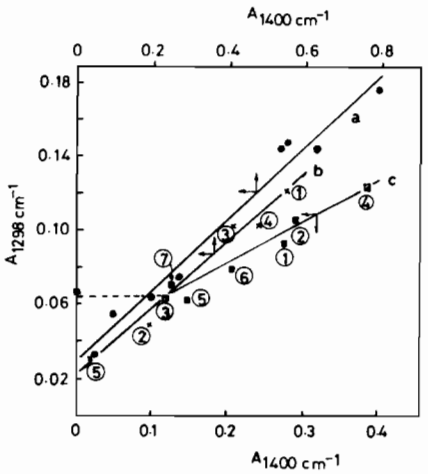

Fig. 2. Change of the IR absorbance of band 1298 cm^{-1} ($A_{1298\,cm^{-1}}$) with the band 1400 cm^{-1} ($A_{1400\,cm^{-1}}$) in $LnCl_3$ doped PA–$[CH(LnCl_3)_y]_x$. (a) *cis*-$(CH)_x$ Ln = Sm; (b) *cis*-$(CH)_x$ Ln = ① La, ② Pr, ③ Gd, ④ Ho, ⑤ Tm, ⑥⑦ Sm; (c) *trans*-$(CH)_x$ as the note in line b.

found that the IR spectra of all fifteen $LnCl_3$ doped PA films are similar irrespective of the different $LnCl_3$ dopants, as shown in Fig. 1a, d.

The absorbance of the 1298 cm^{-1} peak ($A_{1298\,cm^{-1}}$) shows a linear increasing relationship with $A_{1400\,cm^{-1}}$ in $SmCl_3$ doped *cis*-PA films (Fig. 2a) and also *cis*- and *trans*-PA films doped in different $LnCl_3$ species (Fig. 2b, c). As this 1298 cm^{-1} peak is assigned as the in-plane deformation vibration of trans C–H in *trans*-PA by Shirakawa and Ikeda [11], it may be concluded that the isomerization of *cis*-PA to *trans*-PA accompanies the $LnCl_3$ doping process of *cis*-PA. In the case of *trans*-PA, where a weak peak of 1298 cm^{-1} is observed due to the IR vibration saturation by the crystal symmetry of PA, the doping by $LnCl_3$ disturbs the crystal symmetry of PA, which makes the C–H vibration more active in the infrared spectrum.

IR spectra of the doped PA show hydroxyl group absorption at 3450 cm^{-1} and carbonyl group absorptions at 1730 cm^{-1} and 1675 cm^{-1} after oxidation in air. Study of the oxidation kinetics by infrared spectrophotometry indicates that the antioxidation properties of these $LnCl_3$ doped PA films are much better than those of the undoped ones. Detailed results will be published elsewhere [12].

ESR measurements

Only one narrow signal with g value of *ca.* 2.0029 ± 0.0002 can be observed in the ESR spectra of all $LnCl_3$ doped *cis*-PA films, except for $GdCl_3$. This signal has narrower linewidth (ΔH_{pp}) and smaller spin concentration than that of the undoped ones. Some of the ESR results are listed in Table V.

TABLE V. ESR Results of $LnCl_3$ Doped *cis*-PA $[CH(LnCl_3)_y]_x$ [a]

Sample	*cis*-PA	Ln =	La	Sm	Gd	Yb	Y
		y =	0.0214	0.0224	0.0097	0.0024	0.0136
g	2.0028		2.0030	2.0030	2.0029	2.0030	2.0031
ΔH_{pp} (G)	10.93		8.74	9.26	10.93	9.23	7.11
S_1/PA [b]	1		0.547	0.501	0.658	0.503	0.456
S_2/PA [c]	1		0.767	0.723	0.787	0.531	0.529

[a]Doping period: 57 h, measured 4 days after synthesis. [b]S_1/PA represents the relative spin concentration of doped PA to that of the undoped one. [c]S_2/PA represents the relative spin concentration of doped PA in which the weight of dopant was reduced to that of the undoped PA.

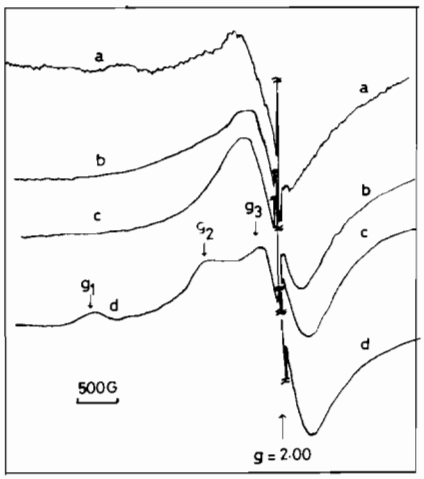

Fig. 3. ESR spectra of *cis*-$[CH(GdCl_3)_y]_x$. (a) y = 0.0097 measured at room temperature (RT); (b) y = 0.0049 (RT); (c) y = 0.0024 (RT); (d) y = 0.0049 (77 K).

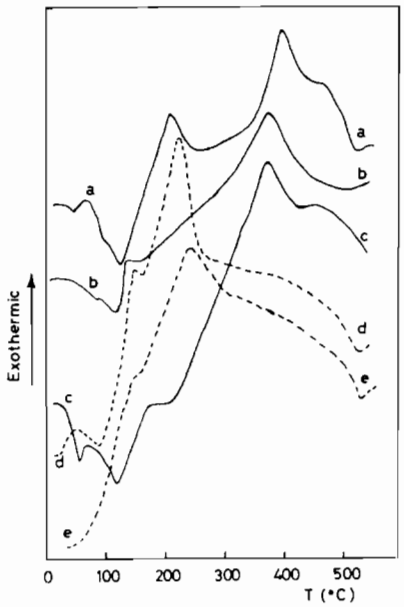

Fig. 4. DSC diagrams of the doped PA. (a) *cis*-$[CH(NdCl_3)_{0.0192}]_x$; (b) *trans*-$[CH(NdCl_3)_{0.0085}]_x$, (c) *trans*-$[CH(LuCl_3)_{0.0263}]_x$; (d) *cis*-$[CH(FeCl_4)_{0.0443}]_x$, (e) *trans*-$[CH(FeCl_4)_{0.0466}]_x$.

ESR spectra of the $GdCl_3$ doped PA measured at room temperature reveal a broad signal in addition to the narrow one (Fig. 3a, b, c). The broad peak, which may arise from the resonance of paramagnetic Gd^{3+} ions in the dopant species, has different g values and linewidths with respect to the different dopant amounts in the doped PA films. When the dopant concentrations (y) of the samples $[CH(GdCl_3)_y]_x$ are 0.0097, 0.0049 and 0.0024, the g values are 2.002, 2.004 and 2.081, and ΔH_{pp}s are 739, 681 and 639 Gauss, respectively.

The ESR spectrum of sample $[CH(GdCl_3)_{0.0049}]_x$ recorded at 77 K shows anisotropic characteristics. The anisotropic g values are as follows: g_1 = 1.986, g_2 = 2.642, g_3 = 6.99 (Fig. 3d). This demonstrates that $GdCl_3$ is somewhat complexed with the PA chain.

DSC and X-ray diffraction study

DSC diagrams of the *cis*- or *trans*-rare-earth PA films doped with $LnCl_3$ (Ln = La, Nd, Sm, Ho, Lu) or $FeCl_3$ were recorded. Two exothermic peaks at 210 °C, 380 °C for $LnCl_3$ doped *cis*-PA or only one exothermic peak at 380 °C for $LnCl_3$ doped *trans*-PA, comparable to those of the undoped *cis*- or *trans*-PA [13], are shown in DSC curves. In addition, there is an endothermic peak at 115–120 °C which is caused by the release of absorbed H_2O in the dopants (Fig. 4a, b, c). In the case of $FeCl_3$ doped PA, where structural change occurred due to doping as confirmed by the X-ray diffraction study [7, 14], only one exothermic peak at 228 °C or 240 °C was found for doped *cis*- or *trans*-PA, respectively (Fig. 4d, e). Comparing the DSC diagrams of the $LnCl_3$ and $FeCl_3$ doped PA films, it is revealed that $LnCl_3$ dopant species have little influence on the structure of the doped PA.

X-ray diffraction diagrams of the doped sample *cis*-$[CH(HoCl_3)_{0.0112}]_x$ and *cis*-$[CH(SmCl_3)_{0.0062}]_x$ show no significant difference from that of the undoped *cis*-PA [7], which is in accord with the above conclusion.

References

1 A. Prón, I. Kulszewicz, D. Billaud and J. Przyluski, *J. Chem. Soc., Chem. Commun.*, 783 (1981).
2 I. Kulszewicz, D. Billaud, A. Prón, P. Bernier and J. Przyluski, *Mol. Cryst. Liq. Cryst., 83*, 159 (1982).
3 J. E. Österholm, H. Isotalo and H. Stubb, *Mol. Cryst. Liq. Cryst., 117*, 107 (1985).
4 D. Boils, F. Schue, J. Sledz and L. Giral, *J. Phys. Colloq.*, 1983 (C3, Conf. Int. Phys. Chim. Polym. Conduct., 1982), 189–92; *Chem. Abstr., 99*:223125q.
5 Z. Shen, M. Yang, Y. Cai and M. Shi, *J. Polym. Sci., Polym. Lett. Ed., 20*, 411 (1982); *Sci. Sin. B, 26*, 785 (1983).
6 M. D. Taylor and C. P. Carter, *J. Inorg. Nucl. Chem., 24*, 387 (1962).
7 Z. Shen, Z. Chen and M. Yang, *Acta Chim. Sin., 44*, 575 (1986).
8 M. D. Taylor, T. T. Cheung and M. A. Hussein, *J. Inorg. Nucl. Chem., 34*, 3073 (1972).
9 K. Rossmanith, *Monatsh. Chem., 100*, 1484 (1969).
10 A. G. MacDiarmid, R. J. Mammone, J. R. Krawczyk and S. J. Porter, *Mol. Cryst. Liq. Cryst., 105*, 89 (1984).
11 H. Shirakawa and S. Ikeda, *Polym. J., 2*, 231 (1971).
12 Z. Chen, Z. Shen, M. Yang and Q. Liu, to be published.
13 M. Yang, Y. Cai, Z. Wang, J. Shen and Z. Shen, *J. Appl. Chem., 1*, 79 (1983) (in Chinese).
14 J. P. Pouget, J. C. Pouxviel, P. Robin, R. Comes, D. Begin, D. Billaud, A. Feldblum, H. W. Gibson and A. J. Epstein, *Mol. Cryst. Liq. Cryst., 117*, 75 (1985).